LETTER OPEN

IMMUNOTHERAPY

Cerebrospinal fluid proteomics exerts predictive potential for immune effector cell-associated neurotoxicity syndrome (ICANS) in CAR-T cell therapy

Tomoko Nomiyama[1,5], Daiki Setoyama[1,5], Ikumi Yamanaka[1], Masatoshi Shimo[2], Kohta Miyawaki[2], Takuji Yamauchi[2], Fumiaki Jinnouchi[2], Teppei Sakoda[2], Kensuke Sasaki[2], Takahiro Shima[2], Yoshikane Kikushige[3], Yasuo Mori[2], Koichi Akashi[2,3], Koji Kato[2,6]✉ and Yuya Kunisaki[1,4,6]✉

Leukemia (2025) 39:983–987; https://doi.org/10.1038/s41375-025-02541-6

TO THE EDITOR:

Chimeric Antigen Receptor (CAR) T-cell therapy is a potent immunotherapy for B cell malignancies, employing genetically engineered T cells to target CD19 [1]. Despite high response rates, it is associated with toxicities like cytokine release syndrome (CRS) and immune effector cell-associated neurotoxicity syndrome (ICANS), which can be life-threatening [2–4]. CRS, the most common adverse event, presents with fever and chills and requires early intervention with Tocilizumab and steroids [3]. ICANS, observed in up to 64% of clinical trial patients [5], manifests as somnolence and cognitive impairment [6, 7]. Risk factors include CRS, high tumor burden, and pre-existing neurological conditions, but reliable biomarkers to predict ICANS severity remain limited, complicating early intervention [8].

The present study retrospectively analyzed residual cerebrospinal fluid (CSF) samples collected prior to CAR-T therapy from 29 patients with B-cell non-Hodgkin lymphoma (Supplementary Tables S1), defining them as an exploratory cohort; Tisagenlecleucel (Tisa-cel, $n = 10$) [9], Axicabtagene ciloleucel (Axi-cel, $n = 12$) [10], and Lisocabtagen maraleucel (Liso-cel, $n = 7$) [11] were used, respectively. Among the 29 enrolled cases, 3 and 8 patients developed grade 1 and grade 2 to 4 ICANS, respectively (grade 1 or higher, categorized as ICANS-positive in this study, Supplementary Table S1) based on the ASTCT Consensus Grading [12] combined with MRI and EEG assessments. All the patients in our first cohort experienced CRS, and ~90% of the patients received tocilizumab and/or corticosteroids, which was not aimed at pre-emptive interventions, before the diagnosis of ICANS. Of the 11 ICANS-positive cases, 7 patients fully recovered from neurological symptoms. However, one case, who developed grade 4 ICANS, resulted in brain death, and the other with grade 2 ICANS died due to lymphoma progression and sepsis (Supplementary Table S2). Although the ICANS incidence rate appears high at 38% (11 out of 29 cases), it might be influenced by the non-random nature of sample collection, which was determined by the availability of residual CSF samples. There were no significant differences in terms of age, gender, CAR-T products, CSF clinical test values including total protein (TP), glucose (Glu), Na, K, LDH, and WBC between two groups. No cases exhibited any signs for active CNS invasion or infections (Supplementary Table S2). Severe CRS (grade 2 and 3) was observed in 28% of ICANS-negative cases and in 63% ICANS-positive cases although the difference was not statistically significant ($p = 0.989$, Fisher's exact test) (Supplementary Table S1).

As the experimental scheme shows (Fig. 1A), CSF proteins were analyzed by data-independent acquisition mass spectrometry (DIA-MS). The total number of proteins identified from all the samples was 1,350, and principal component analysis (PCA) was performed using the protein profiles. The PCA score plot identified one sample as an "outlier" that exhibited an extraordinal shift from the other samples (Supplementary Fig. S1A). The case showed an abnormally high total protein level as a value of 498 mg/dL, likely causing an artifact in the mass spectrometry measurement and a significant reduction in the number of identified proteins (Supplementary Fig. S1B). We then performed partial least squares discriminant analysis (PLS-DA) with 28 samples excluding the case, to discriminate the two groups of patients with and without ICANS. A model constructed using score plots was able to separate the two groups (Supplementary Fig. 1B) and the contribution of each factor to this model is reflected in the VIP score (Supplementary Table S3). The top 30 factors contributing to the first component (Comp1) are visualized in a heat map (Fig. 1C). For the top 100 factors contributing to both the first and second components, STRING analysis was performed to visualize the network among proteins to clarify their biological roles, and they were divided into five clusters by the k-means method (Fig. 1D). In addition, the factors in each cluster were subjected to Gene Ontology (GO) enrichment analysis (Supplementary Table S4). These clusters were annotated to biological pathways (Fig. 1D)

[1]Department of Clinical Chemistry and Laboratory Medicine, Kyushu University Hospital, Fukuoka, Japan. [2]Department of Medicine and Biosystemic Science, Graduate School of Medical Sciences, Kyushu University, Fukuoka, Japan. [3]Center for Cellular and Molecular Medicine, Kyushu University Hospital, Fukuoka, Japan. [4]Department of Clinical Chemistry and Laboratory Medicine, Graduate School of Medical Sciences, Kyushu University, Fukuoka, Japan. [5]These authors contributed equally: Tomoko Nomiyama, Daiki Setoyama. [6]These authors jointly supervised this work: Koji Kato, Yuya Kunisaki. ✉email: kato.koji.429@m.kyushu-u.ac.jp; kunisaki.yuya.519@m.kyushu-u.ac.jp

Received: 1 September 2024 Revised: 15 January 2025 Accepted: 12 February 2025
Published online: 11 March 2025

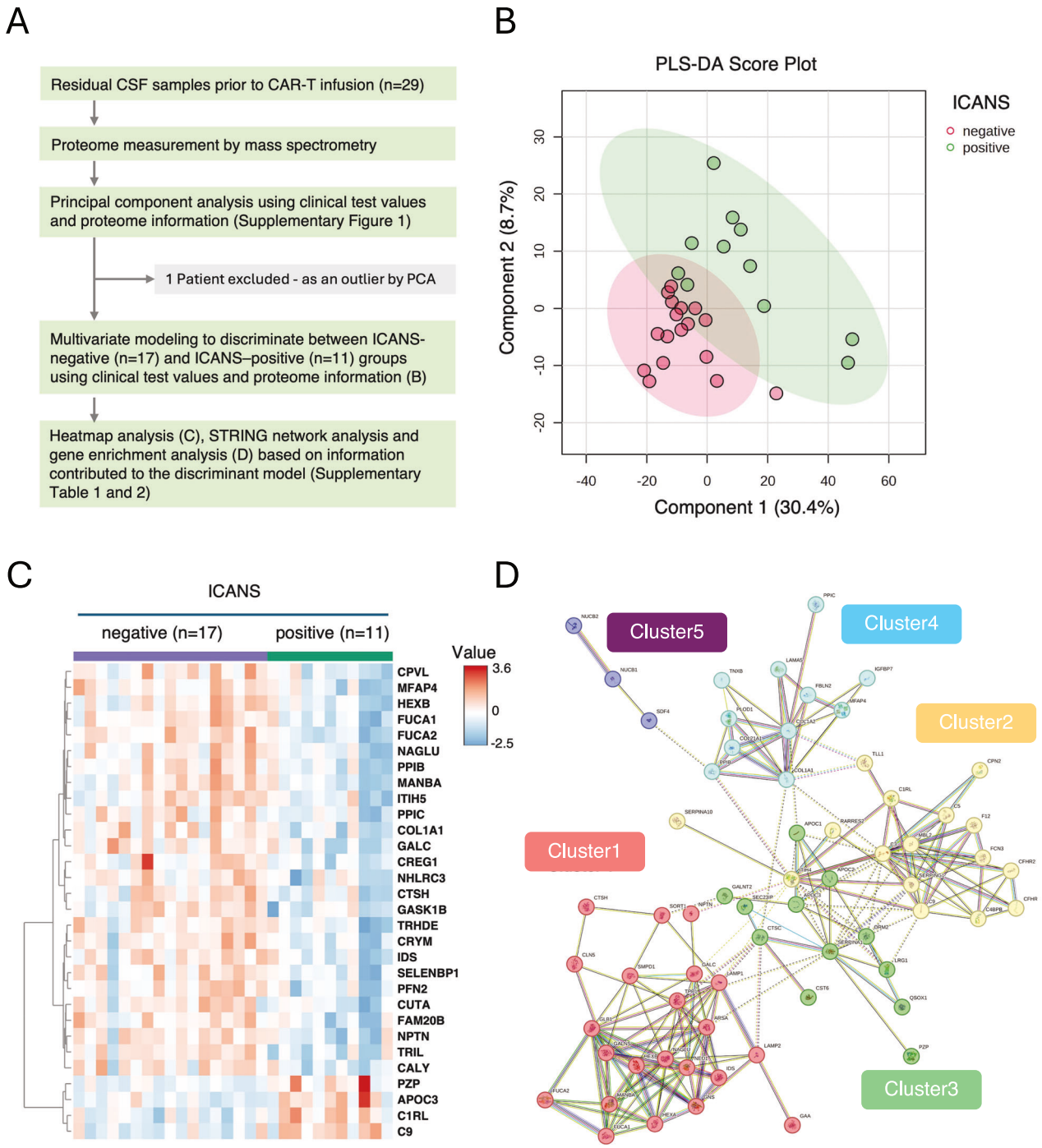

Fig. 1 Cerebrospinal fluid (CSF) protein profiling and biological process extraction related to ICANS occurrence. A Proteomics and statistics workflow. **B** The data obtained from CSF proteomics and clinical test values were subjected to supervised partial least square discriminant analysis (PLS-DA) to classify the presence or absence of ICANS. The PLS-DA score plot demonstrated the separation between ICANS-positive ($n = 11$, green) and ICANS-negative ($n = 18$, red) groups, with the first two latent variables accounting for 30.4% (Component 1) and 8.7% (Component 2) of the total variance. Each dot represents an individual, and the ellipses correspond to the 95% confidence intervals for each group. **C** The top 30 factors contributing to the first and second components in (**B**) are visualized in a clustered heatmap. **D** The top 100 protein contributors were subjected to STRING network analysis and classified into five clusters using the k-means method. Each cluster was annotated with biological processes by gene ontology analysis (Supplementary Table S3). Cluster 1: Carbohydrate derivative catabolic process. Cluster 2: Complement activation. Cluster 3: Chylomicron remnant clearance. Cluster 4: Extracellular matrix.

such as hydrolytic enzyme functions acting on lysosomes or glycosyl bonds (Cluster 1), complement activation or humoral immunity (Cluster 2), LDL particle clearance (Cluster 3), and extracellular matrix (Cluster 4), suggesting their involvement in the development of ICANS. Notably, proteins belonging to Cluster 2, including C1RL, C3, C4BPB, C5, and C9, which are integral to complement activation, exhibited elevation in the ICANS-positive group (Supplementary Fig. S2).

Next, we employed a strategy to find highly sensitive biomarkers to predict the occurrence of ICANS shown in the scheme (Fig. 2A). Among the 864 proteins identified commonly in all the samples, 46 proteins were screened as candidate factors

A

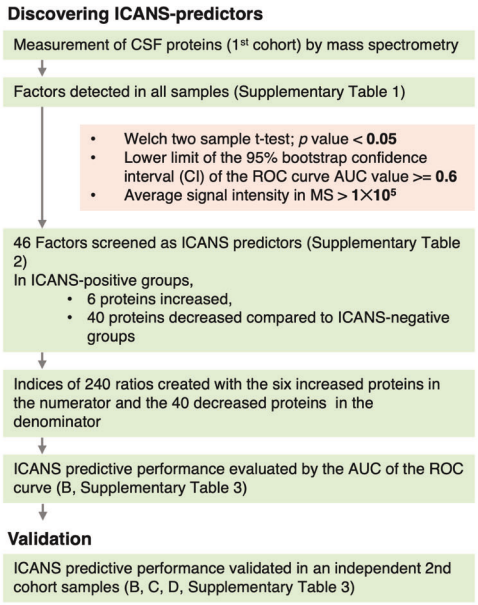

B

Phase	Rank	Ratio Factor		AUC	95% CI	
		Numerator	Denominator		Above	Below
1st Cohort n=29	1	C1RL	FUCA2	0.95	0.83	1.00
	7	F12	FUCA2	0.92	0.78	0.99
	23	C1RL	CPVL	0.89	0.75	0.99
	38	C9	CPVL	0.90	0.74	1.00
	54	F12	CPVL	0.89	0.73	1.00
2nd Cohort n=10	3	C1RL	FUCA2	1.00	0.81	1.00
	5	F12	FUCA2	1.00	0.71	1.00
	6	C1RL	CPVL	1.00	0.71	1.00
	4	C9	CPVL	1.00	0.71	1.00
	2	F12	CPVL	1.00	0.81	1.00

C

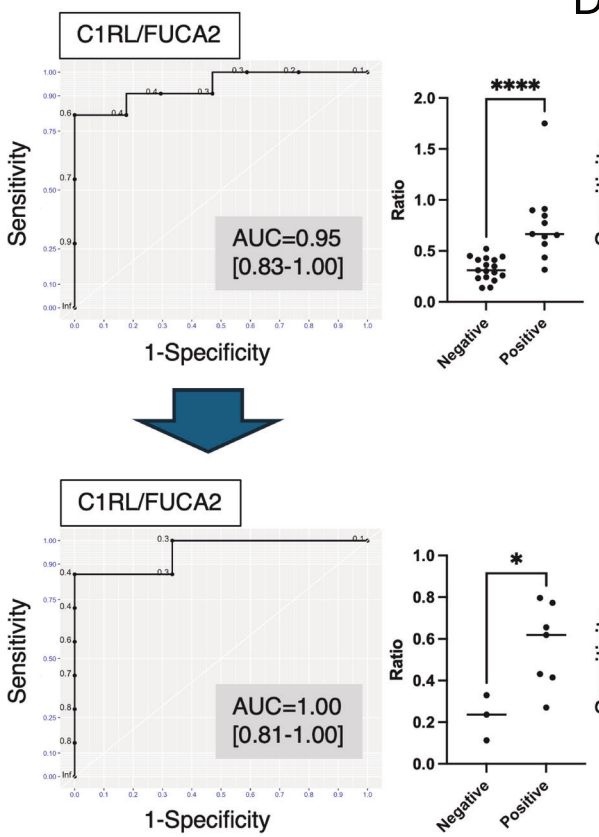

D

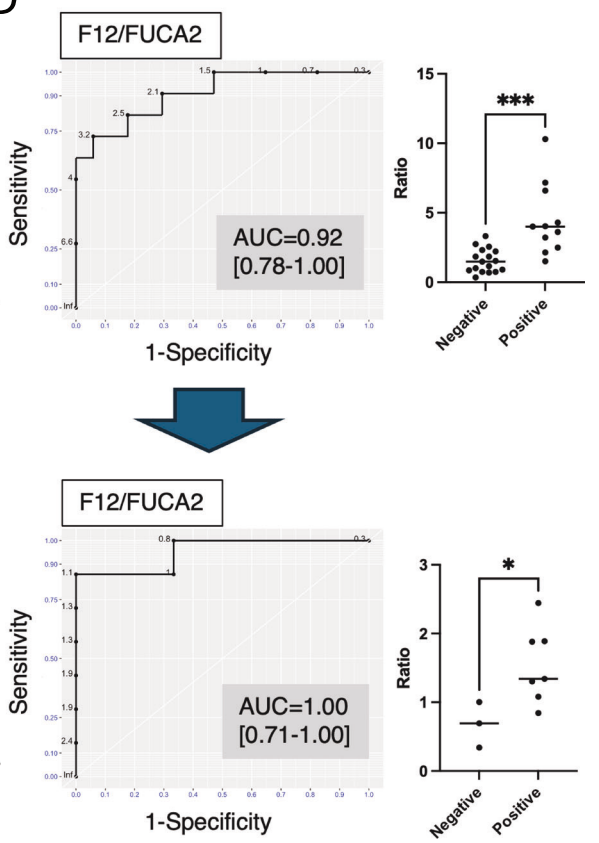

(Supplementary Table S5) that met our criteria of signal intensity thresholds ($>1 \times 10^5$), single discriminant performance criteria (AUC ≥ 0.6) (Supplementary Table S6), and *p*-values of t-test ($p < 0.05$). Of these, 6 factors were increased in the ICANS-positive group, while the remaining 40 were decreased. Therefore, a composite ratio index (increased factor to decreased one) was calculated, and its potential to discriminate between the ICANS-positive and negative groups was evaluated along with its stand-alone performance (Fig. 2B, Supplementary Table S7). There were 19 ratio factors with AUC values above 0.9, among which the composite ratio of C1RL and FUCA2 discriminated ICANS-positive and negative groups the most efficiently with an AUC value of 0.95 (95% confidence interval of 0.83–1.0) for the ROC curve (Fig. 2C).

Fig. 2 Screening for ICANS-predictors and validation of their predictive performance. A A scheme of exploration and validation of predictive biomarkers for ICANS. Among the proteins detected in the CSF proteomics of the exploratory cohort, 46 proteins met the criteria; signal intensity thresholds (1×10^5), single discriminant performance criteria (AUC > 0.6, Supplementary Table S4), and p-values of t-test (p value < 0.05) were identified, detailed in Supplementary Table S5. A composite ratio was created with the amounts of two proteins in the ICANS-positive group, by placing elevated one in the numerator and decreased one in the denominator. A receiver operating characteristic (ROC) curve was created to classify the presence or absence of ICANS. Selected ratio factors were applied to the CSF proteomics of the second cohort and their performance was evaluated. **B** The top 5 high-performance ratio factors validated in the second cohort. The 95% confidence interval (95% CI) for the AUC was calculated using the bootstrap method with 1000 iterations of repeated stratified replicates. **C** The ROC curves for the ratio factors of C1RL and FUCA2 in the first cohort (top) and the second cohort (bottom), and dot plots of the ratio between the two groups are shown. Asterisk * indicates a p-value of less than 0.05, *** indicates a p-value of less than 0.001, and **** indicates a p-value of less than 0.0001. **D** The ROC curves for the ratio factors of F12 and FUCA2 and the dot plots were shown as in **C**.

To validate the ratio factors identified with the initial cohort, we examined an extended cohort ($n = 10$, including 7 ICANS-positive and 3 ICANS-negative subjects, Supplementary Table S1), which comprised CSF samples collected from the different department at the same hospital, and no participants overlapped between the cohorts. The ratio factors were assessed for their ability to distinguish between the two groups using ROC curves (Fig. 2B). The C1RL/FUCA2 ratio factor, which exhibited the best performance in the initial cohort, achieved an AUC of 1.0 (95% CI: 0.81–1.0), and the F12/FUCA2 ratio factor also demonstrated a strong performance with an AUC (95% CI: 0.71–1.0), confirming the reliability of these biomarkers to predict the occurrence of ICANS. Both ratio values were significantly elevated in the positive group compared to the negative group (Fig. 2C, D). Previously, serum levels of neurofilament light chain (NfL) [13] and plasma fibrinogen [6] were reported as biomarkers for assessing the risk and severity of ICANS. However, their discriminative abilities appeared to be modest, with AUC values of 0.71 for NfL and 0.724 for fibrinogen, respectively. In contrast, the CSF biomarkers investigated in this study exhibited remarkable performance with an AUC of 0.95, significantly outweighing previously reported biomarkers. The issue of whether our CSF biomarkers correlate with blood levels remains unaddressed. Identifying blood biomarkers that correlate with and are comparable to the CSF biomarkers may facilitate the development of more non-invasive and convenient laboratory testing methods.

To investigate the molecular mechanisms underlying ICANS pathogenesis (Supplementary Fig. S3A), PLS-DA was performed on 10 samples from the second cohort, revealing clear group separation (Supplementary Fig. S3B). Contributing factors from the first component (Supplementary Table S3) identified 153 shared between the two cohorts (Supplementary Fig. S3C, Supplementary Table S8). A STRING network GO analysis identified three significant clusters (Supplementary Fig. S3D–G, Supplementary Table S4), notably cluster 2 (Supplementary Fig. S3F), which highlighted complement activation involving C1RL and other complement factors (Supplementary Fig. S2). There findings suggest that complement pathway activation plays a role in ICANS pathogenesis and represent a potential therapeutic target. Further analysis is needed to clarify the contributions of these factors and pathways, with emerging complement-targeting drugs offering a promising avenue for treatment [14].

Several studies have reported variations in the incidence of ICANS among different CAR-T products [4, 9–11]. To address the possibility that protein profiles or risk factors may differ depending on the CAR-T products used, we conducted an additional analysis to explore these differences, while acknowledging the limitations of the small sample size. We reanalyzed the CSF proteomics profiles in the first cohort, stratified by CAR-T product types. The PCA score plot revealed no distinct clustering corresponding to the three CAR-T products (Supplementary Fig. S4A), and ANOVA analysis identified no significant differences in protein abundance among the groups (Supplementary Fig. S4B). Moreover, biomarker performance of the C1RL/FUCA2 and F12/FUCA2 ratio factors remained still high within both the Axi-cel and non-Axi-cel sub-cohorts (Supplementary Fig. S4C). While these results suggest that differences of the CAR-T products do not substantially influence the performance of the identified biomarkers, further studies with larger sample sizes are needed to confirm these findings.

Increasing evidence suggests that myeloid cells contribute to the pathogenesis of ICANS following CAR T-cell therapy. In our analysis, CSF nuclear cell counts in all the cases were normal (1-2 cells/μL), preventing identification of the dominant cell type. However, previous studies report increased CD14+ myeloid cells in severe ICANS [15], highlighting the need to explore their role in its pathophysiology in future studies.

Given the retrospective nature and small sample size of this study, a prospective trial with a larger cohort is needed to confirm the findings, explore differences among CAR-T products, and validate biomarker accuracy in relation to ICANS severity. In conclusion, our study identifies highly discriminatory CSF biomarkers for ICANS prediction, offering insights into its pathogenesis and the potential to optimize CAR-T therapy by enhancing efficacy and reducing adverse effects.

DATA AVAILABILITY

Our proteomics data have been deposited in the ProteomeXchange Consortium and the jPOST partner repository (https://repository.jpostdb.org/). The accession numbers are PXD052238 for ProteomeXchange and JPST003107 for jPOST.

REFERENCES

1. Kochenderfer JN, Feldman SA, Zhao Y, Xu H, Black MA, Morgan RA, et al. Construction and Preclinical Evaluation of an Anti-CD19 Chimeric Antigen Receptor. J Immunother. 2009;32:689–702.
2. Deng Q, Han G, Puebla-Osorio N, Ma MCJ, Strati P, Chasen B, et al. Characteristics of anti-CD19 CAR T cell infusion products associated with efficacy and toxicity in patients with large B cell lymphomas. Nat Med. 2020;26:1878–87.
3. Morris EC, Neelapu SS, Giavridis T, Sadelain M. Cytokine release syndrome and associated neurotoxicity in cancer immunotherapy. Nat Rev Immunol. 2022;22:85–96.
4. Yang C, Nguyen J, Yen Y. Complete spectrum of adverse events associated with chimeric antigen receptor (CAR)-T cell therapies. J Biomed Sci. 2023;30:1–18.
5. Schubert ML, Schmitt M, Wang L, Ramos CA, Jordan K, Müller-Tidow C, et al. Side-effect management of chimeric antigen receptor (CAR) T-cell therapy. Ann Oncol. 2021;32:34–48.
6. Holtzman NG, Xie H, Bentzen S, Kesari V, Bukhari A, El Chaer F, et al. Immune effector cell-Associated neurotoxicity syndrome after chimeric antigen receptor T-cell therapy for lymphoma: Predictive biomarkers and clinical outcomes. Neuro Oncol. 2021;23:112–21.
7. Tedesco VE, Mohan C. Biomarkers for Predicting Cytokine Release Syndrome following CD19-Targeted CAR T Cell Therapy. J Immunol. 2021;206:1561–8.
8. Levstek L, Janžič L, Ihan A, Kopitar AN. Biomarkers for prediction of CAR T therapy outcomes: current and future perspectives. Front Immunol. 2024;15:1–19.
9. Schuster SJ, Bishop MR, Tam CS, Waller EK, Borchmann P, McGuirk JP, et al. Tisagenlecleucel in Adult Relapsed or Refractory Diffuse Large B-Cell Lymphoma. N Engl J Med. 2019;380:45–56.
10. Locke FL, Miklos DB, Jacobson CA, Perales M-A, Kersten M-J, Oluwole OO, et al. Axicabtagene Ciloleucel as Second-Line Therapy for Large B-Cell Lymphoma. N Engl J Med. 2022;386:640–54.

11. Kamdar M, Solomon SR, Arnason J, Johnston PB, Glass B, Bachanova V, et al. Lisocabtagene maraleucel versus standard of care with salvage chemotherapy followed by autologous stem cell transplantation as second-line treatment in patients with relapsed or refractory large B-cell lymphoma (TRANSFORM): results from an interim analysis. Lancet. 2022;399:2294–308.
12. Lee DW, Santomasso BD, Locke FL, Ghobadi A, Turtle CJ, Brudno JN, et al. ASTCT Consensus Grading for Cytokine Release Syndrome and Neurologic Toxicity Associated with Immune Effector Cells. Biol Blood Marrow Transplant. 2019;25:625–38.
13. Schoeberl F, Tiedt S, Schmitt A, Blumenberg V, Karschnia P, Burbano VG, et al. Neurofilament light chain serum levels correlate with the severity of neurotoxicity after CAR T-cell treatment. Blood Adv. 2022;6:3022–6.
14. Mastellos DC, Ricklin D, Lambris JD. Clinical promise of next-generation complement therapeutics. Nat Rev Drug Discov. 2019;18:707–29.
15. Siegler EL, Kenderian SS. Neurotoxicity and Cytokine Release Syndrome After Chimeric Antigen Receptor T Cell Therapy: Insights Into Mechanisms and Novel Therapies. Front Immunol. 2020;11:1–11.

ACKNOWLEDGEMENTS

This study was partly supported by Grants-in-Aid for Scientific Research from the Japan Society for the Promotion of Science (grants 21H02950 to YK). We would like to thank Momoko Asakawa and Ayumi Inayoshi for their assistance with the research, Shiho Taniguchi, Kyohei Mori, Naoko Ban, and Miyuki Yoshikawa for their management and provision of clinical information.

AUTHOR CONTRIBUTIONS

TN, DS and YK designed the study; TN and IY collected the clinical samples and patients' data; TN and DS collected and analyzed the data; TN, DS, and YK interpreted the data; TN and IY drafted the manuscript; DS, KA, KK, and YK revised the manuscript. IY, MS, KM, TY, FJ, TS, KS, TS, YK, YM, KA, and KK provided clinical feedback. All authors approved the manuscript.

COMPETING INTERESTS

The authors declare no competing financial interests related to this study. Koji Kato; Honoraria: AbbVie, Bristol-Myers Squibb, Chugai, Dainippon-Sumitomo, Janssen, Kyowa Kirin, MSD, AbbVie, Ono, Gilead Sciences, Novartis; Consulting or Advisory Role: AbbVie, AstraZeneca, Chugai, Daiichi Sankyo, Eisai, Janssen, Bristol-Myers Squibb, Novartis, Gilead Sciences; Research Funding: AbbVie, Astellas, MSD, Bristol-Myers Squibb, Chugai, Daiichi Sankyo, Eisai, Janssen, Kyowa Kirin, Novartis, Ono, Gilead Sciences. All conflicts of interest declared are unrelated to the content of this manuscript.

ETHICS APPROVAL AND CONSENT TO PARTICIPATE

This study was a retrospective analysis conducted in accordance with the principles outlined in the Declaration of Helsinki and was approved by the Ethics Committee of Kyushu University (IRB numbers: 22213 and 23399). Informed consent was obtained using an opt-out methodology, whereby study details were disclosed on the institutional website, allowing participants the opportunity to decline participation. Data and CSF samples from individuals who did not opt out were included in the analysis. All collected data were anonymized prior to analysis to safeguard the privacy of participants.

ADDITIONAL INFORMATION

Supplementary information The online version contains supplementary material available at https://doi.org/10.1038/s41375-025-02541-6.

Correspondence and requests for materials should be addressed to Koji Kato or Yuya Kunisaki.